Biogeosciences Discuss., 8, 185–220, 2011
www.biogeosciences-discuss.net/8/185/2011/
doi:10.5194/bgd-8-185-2011

Biogeosciences Discussions

The impact of anticyclonic mesoscale structures on microbial food webs in the Mediterranean Sea

U. Christaki[1], F. Van Wambeke[2], D. Lefevre[2], A. Lagaria[1,3], L. Prieur[4], M. Pujo-Pay[5,6], J.-D. Grattepanche[1], J. Colombet[7], S. Psarra[3], J. R. Dolan[8], T. Sime-Ngando[7], P. Conan[5,6], M. G. Weinbauer[8], and T. Moutin[9]

[1]INSU-CNRS, UMR 8187, LOG, Laboratoire d'Océanologie et des Géosciences, Université Lille Nord de France, ULCO, 32 avenue Foch, 62930 Wimereux, France
[2]INSU-CNRS, UMR 6117, LGEM, Laboratoire de Microbiologie, Géochimie et Ecologie Marines,Université de la Méditerranée, Centre d'Océanologie de Marseille, Campus de Luminy Case 901, 13 288 Marseille cedex 9, France
[3]Hellenic Centre for Marine Research, Inst. of Oceanography, 71003 Heraklion, Crete, Greece
[4]INSU-CNRS, UMR 7094, LOV, Laboratoire d'Océanographie de Villefranche sur Mer, Université Pierre et Marie Curie, Port de la darse, 06238 Villefranche sur Mer, France
[5]INSU-CNRS, UMR 7621, Laboratoire d'Océanographie Microbienne, Observatoire Océanologique, 66651 Banyuls/mer, France

[6]UPMC Univ Paris 06, UMR 7621, Laboratoire d'Océanographie Microbienne, Observatoire Océanologique, 66651 Banyuls/mer, France
[7]INSU-CNRS, UMR 6023, LMGE, Laboratoire Microorganismes: Génome et Environnement, 63177 Aubière cedex, France
[8]INSU-CNRS, UMR 7093, LOV, Microbial Ecology and Biogeochemistry, Université Paris6 CNRS UMR7093, Station Zoologique, B.P. 28, Villefranche-sur-Mer 06230, France
[9]INSU-CNRS, UMR 6535, LOPB, Laboratoire d'Océanographie physique et biogéochimique Université de la Méditerranée, Centre d'Océanologie de Marseille, Campus de Luminy Case 901, 13 288 Marseille cedex 9, France

Received: 6 December 2010 – Accepted: 8 December 2010 – Published: 10 January 2011

Correspondence to: U. Christaki (urania.christaki@univ-littoral.fr)

Published by Copernicus Publications on behalf of the European Geosciences Union.

Abstract

The abundance and activity of the major members of the heterotrophic microbial community – from viruses to ciliates – were studied along a longitudinal transect across the Mediterranean Sea in the summer of 2008. The Mediterranean Sea is characterized by a west to the east gradient of deepening of DCM (deep chlorophyll maximum) and increasing oligotrophy reflected in gradients of heterotrophic microbial biomass and production. However, within this longitudinal trend, hydrological mesoscale features exist and likely influence microbial dynamics. We show here the importance of mesoscale structures by a description of the structure and function of the microbial food web through an investigation of 3 geographically distant eddies within a longitudinal transect. Three selected sites each located in the center of an anticyclonic eddy were intensively investigated: in the Algero-Provencal Basin (St. A), the Ionian Basin (St. B), and the Levantine Basin (St. C). The 3 geographically distant eddies showed the lowest values of the different heterotrophic compartments of the microbial food web, and except for viruses in site C, all stocks were higher in the neighboring stations outside the eddies. During our study the 3 eddies showed equilibrium between GCP (Gross Community Production) and DCR (Dark Community Respiration); moreover, the west-east (W-E) gradient was evident in terms of heterotrophic biomass but not in terms of production. Means of integrated PPp values were higher at site B (~190 mg C m^{-2} d^{-1}) and about 15% lower at sites A and C (~160 mg C m^{-2} d^{-1}). Net community production fluxes were similar at all three stations exhibiting equilibrium between gross community production and dark community respiration.

1 Introduction

The Mediterranean Basin is one of the most oligotrophic marine systems in the world. The basin-wide cyclonic circulation of nutrient-depleted water (Dugdale and Wilkerson, 1988), hot, dry climate and low land run-off contribute to the low productivity of the sea. The Mediterranean also exhibits a marked west to east gradient of oligotrophy

seen in an increasing nutrient depletion from west to east (Krom et al., 1993), declines in chlorophyll concentrations (Moutin and Raimbault, 2002; Ignatiades et al., 2009) and rates of primary production (Turley et al., 2000). The hypothesis of phosphorus limitation of primary production in the Mediterranean has inspired numerous studies dealing with microbial processes in its open waters and resulted in the establishment of large-scale patterns of abundance and activity for different planktonic food web components (reviewed in Siokou et al., 2010). The Mediterranean is generally considered as an oligotrophic ecosystem characterized by a microbially dominated food web. The dominance of small heterotrophs and small phototrophs in this region is consistent with a scenario of little energy transfer to the higher trophic levels (cf. review by Siokou et al. 2010). It appears that microbial heterotrophic activity is a dominant energy pathway in the planktonic food web in particular in the Eastern Mediterranean, that the food web does not act as a significant carbon sink since most of the organic carbon produced is consumed and respired (Regaudie-de-Gioux et al., 2009). Up to 90–95% of primary production is sustained by internal recycling of organic matter during the stratifed period (Moutin and Raimbault, 2002). Turley et al. (2000) hypothesized that a large portion of primary production is directly channeled to heterotrophic prokaryotes through exudation and/or lysis by nutrient-stressed phytoplankton. Probably the most convincing evidence of P limitation of heterotrophic prokaryotes resulted from the CYCLOPS in situ P-fertilization experiment conducted in May 2002 in the Cyprus Eddy. In this experiment, prokaryotic heterotrophic production increased in response to P addition whereas phytoplankton biomass diminished (Thingstad et al., 2005).

Nonetheless, the Mediterranean Sea while often attributed the label “oligotrophic”, shows considerable variability over a wide range of temporal and spatial scales. This variability is reflected in the microbial components of the planktonic food web. For example, in the west the Almeria-Oran front is an area of high primary production (Videau et al., 1994; Van Wambeke et al., 2004) compared to surrounding waters, while the Cyprus eddy in the east is a zone of low phytoplankton production (Psarra et al., 2005).

One of the central ideas of the BOUM cruise (Biogeochemistry from Oligotrophic to the Ultra-oligotrophic Mediterranean) in summer 2008, was that, besides the general aspect of oligotrophy in the Mediterranean, the mesoscale discontinuities likely influence biological processes. For this purpose, during the BOUM cruise a particular sampling effort was made within 3 major anticyclonic eddies along a W-E transect (Fig. 1).

In this study, our first objective was a general description of the vertical and spatial distribution of the microbial food web and in particular its heterotrophic part – along a W-E transect of 17 stations. Our second objective was to characterize the function and the relative contribution of the microbial food web to the cycling of organic matter within 3 geographically distant anticyclonic mesoscale eddies. Our hypothesis was that the impact of the eddies will be recognizable within the broader W-E gradient of oligotrophy. The major biogeochemical and biological parameters reported in this study are microbial stocks (from viruses to ciliates), primary production, heterotrophic prokaryotic production and oxygen fluxes (community production and respiration).

2 Methods

2.1 Sample collection, general characteristics of the study site

The BOUM cruise was carried out from 16 June to 20 July 2008. Biological data presented in this study are based on surface-layer sampling (8–10 depths from 0 to 200 m) of 17 stations along a longitudinal transect from the Levantine Basin (34° E) to the Western Basin (5° E, Fig. 1). Fourteen representative "short duration" stations (2–3 h occupation), and at three selected "long duration" sites (3 days occupation) within anticyclonic eddies were studied. Profiles of temperature, conductivity, oxygen and fluorescence were obtained using a Sea-Bird Electronics 911 PLUS Conductivity-Temperature Depth (CTD) and water samples using Niskin bottles with Teflon-coated springs and O-rings. Total chlorophyll-*a* (Chl-*a*=chlorophyll-*a* plus divinyl-chlorophyll-*a*)

was measured by High Performance Liquid Chromatography with methodology described in Ras et al. (2008). Concentrations of NO_3+NO_2 and soluble reactive phosphorus, referred to the term phosphate (PO_4) in this paper, were immediately measured on board with an autoanalyser (Bran+Luebbe autoanalyser II) according to the colorimetric method (Tréguer and Le Corre, 1975), as fully described in Pujo-Pay et al. (2010).

2.2 Abundance of microbial components

Virus-like particles (VLP) and heterotrophic bacterial abundances (HBA, *sensus stricto* heterotrophic bacteria+archaea) were determined by flow cytometry. Subsamples (2 ml) were fixed with glutaraldehyde (final concentration, 0.5%), refrigerated for 10–20 min, frozen in liquid nitrogen and stored at −80°C (Marie et al., 1999) until analyzed. Counts were made using a FACSCalibur flow cytometer (BD Sciences, San Jose, CA, USA) equipped with an air-cooled laser providing 15 mW at 488 nm with the standard filter set-up. Virus and procaryotes were stained with SYBRGreen I as described in detail in Marie et al. (1999) and Brussaard (2004). Populations of prokaryotes and viruses differing in fluorescence intensity were distinguished on plots of side scatter versus green fluorescence (530 nm wavelength, fluorescence channel 1 of the instrument). FCM list modes were analyses using CellQuest Pro software (BD Biosciences, version 4.0). HBA was converted to biomass using a carbon conversion factor of 12 fg C cell^{-1} (Fukuda et al., 1998).

To enumerate heterotrophic nanoflagellates (HNF), samples (20–30 ml) were preserved using formaldehyde (final concentration of 1%). Samples were filtered onto black Nuclepore filters (pore size, 0.8 µm) and stained with DAPI (Porter and Feig, 1980) within 5 h of sampling and stored at −20°C until counting. HNF were enumerated using a LEITZ DMRB epifluorescence microscope at 1000 ×. To distinguish between autotrophic and heterotrophic nanoflagellates, autofluorescence (chlorophyll) was determined under blue light excitation.

For ciliate enumeration, samples (500 ml) were placed in opaque glass bottles and fixed with acid Lugol's solution (final concentration, 2%). The samples were stored at 4°C in the dark until analysis (max. 3 months later). The fixed samples were allowed to settle for 3 days then the supernatant gently removed yielding ~100 ml of concentrate which was further sedimented in 100 ml Hydrobios chambers for at least 24 h. Ciliate enumeration was done using a Nikon Eclipse TE2000-S inverted microscope, the whole chamber was examined at 400x. Ciliates were distinguished as aloricate, naked ciliates comprising taxa of the subclasses Choreotrichida and Oligotrichia and tintinnids of the subclass Choreotrichida, order Tintinnida (Lynn, 2008). Ciliates were grouped into 4 size groups (<20, 20–30, 30–50, >50 µm). Biovolumes of all taxa and morphotypes identified in this study were calculated using the linear dimensions of cells. Biovolumes were converted to biomass using volume-to-carbon conversion factors of 190 fg C μm^{-3} for Lugol's preserved samples (Putt and Stoecker, 1989).

2.3 Bacterial production

"Bacterial" production (BP – *sensu stricto* referring to heterotrophic prokaryotic production –) was estimated by the ^{3}H-leucine method at 9 depths in the 0–200 m water column. At each depth, 1.5 ml duplicate samples and a control were incubated with a mixture of L-[4,5-^{3}H] leucine (Perkin Elmer, specific activity 115 Ci $mmol^{-1}$) and non-radioactive leucine at final concentrations of 16 and 7 nM, respectively. Samples were incubated in the dark at in situ temperature, fixed and treated following the microcentrifugation protocol (Smith and Azam, 1992) as described in detail in Van Wambeke et al. (2010) and using a conversion factor of 1.5 kg C per mole leucine incorporated.

2.4 Primary production

Carbon fixation estimates using the ^{14}C method according to the experimental protocol detailed by Moutin and Raimbault (2002) were carried out using an in situ rig at stations A, B and C during the first and the third day of station occupation. Samples were

collected before sunrise using 12 L Niskin bottles and dispensed into 320 ml polycarbonate bottles, 3 light and one dark sample per depth, for each of 10 depths covering the euphotic zone and inoculated with 20 µCi of $NaH^{14}CO_3$ (Amersham, CFA3). Three samples were filtered immediately after inoculation for T_0 determination, and 250 µl of sample was taken at random from 3 bottles and stored with 250 µl of ethanolamine to determine the quantity of added tracer (Q_i). Then, the bottles were incubated in situ in a drifting in situ rig for 24 h (dawn-to-dawn). After recovery of the rig, the samples were filtered on GF/F filters under low vacuum pressure (200 mmHg) to measure net absorption (A_N mgC m^{-3}). Filters were then flooded with 500 µl of HCl 0.5 M and stored for counting at the laboratory. In the laboratory, samples were dried over 12 h at 60°C, the 10 ml of ULTIMAGOLD-MV scintillation fluo (Packard) were added to the filters and dpm was counted after 24 h with a Packard Tri carb 2100 TR liquid scintillation analyzer. Daily (24 h dawn-to-dawn) particulate primary production (PPp) was obtained from the difference between light and dark bottles measurements. Integrated particulate primary production PPp (mg m^{-2} d^{-1}) was calculated assuming: 1) that subsurface (about 5 m) rates are identical to surface rates (not measured); and 2) that rates are zero at 20 m below the deepest sampled depth (below the photic zone). The total integrated primary production (PP_{total}) was calculated from PPp and a percentage of extracellular release (PER), with PER defined as the percentage of dissolved primary production relative to the sum of particulate and dissolved primary production. PER was determined from on-board incubated samples (Lopez-Sandoval et al. 2010). They sampled sea water for such measurements at selected depths from a CTD the CTD cast used for the 24 h-long in situ incubations (the first and the third day of each site occupation). We used the integrated data of particulate (PP_p) and dissolved primary production (PP_d) determined on their profiles to compute an averaged PER for each profile. Then we used this percentage to our own data set as follows:

$$PP_{total} = PP_p/(1 - PER) \quad (1)$$

2.5 Biological oxygen fluxes

Rates of gross community production (GCP), dark community respiration (DCR) and net community production (NCP) were estimated from changes in the dissolved oxygen concentration over 24 h incubations carried out on the in situ rig at stations A, B and C during the first and the third day of station occupation. Rates were measured at up to 9 depths of decreasing irradiance (75, 55, 35, 20, 10, 7, 3, 1, 0%), to encompass the euphotic zone. The 0% irradiance samples corresponded to 130, 160 and 147 m depth for A, B and C, respectively. For each depth, three sets of four replicate water samples were placed into 125 ml borosilicate glass bottles. The first set of samples was fixed immediately (using Winkler reagents) to measure oxygen concentrations at time 0; the second set placed in darkened bottles and the third set in transparent bottles. The samples from the last two sets were placed on an in situ rig, for incubation at the depth of sample origin, and incubated for 24 h, from dawn to dawn. Dissolved oxygen concentration was measured using an automated high-precision Winkler titration system linked to a photometric end point detector (Williams and Jenkinson, 1982). NCP was calculated as the difference in the dissolved oxygen concentration between "light" incubated samples and "time 0" samples. DCR was calculated as the difference between "dark" incubated samples and "time 0" samples. DCR rates are expressed as a negative O_2 flux. GCP is the difference between NCP and DCR. Results presented in this study are data integrated over 130 m (site A), 160 m (site B) and145 m (site C). Standard errors of the rates are calculated from the standard deviation of quadruple samples sets. The mean standard error obtained was ± 0.3 mmol O_2 m^{-3} d^{-1}. The DCR was converted into CO_2 units applying a respiratory quotient of 0.8 (Lefèvre et al., 2008 and references therein) GCP was converted to carbon units applying a photosynthetic quotient (PQ) of 1.4 (Laws, 1991).

3 Results

3.1 General and longitudinal features

The water column was characterized by the presence of the seasonal thermocline. Fluorescence profiles during the cruise indicated a distinct deep chlorophyll maximum (DCM, Table 1). The fluorescence maximum depth declined from 30 m at the furthest west (NW Mediterranean, St. 27) to 120 m at the furthest east (Levantine Basin, St. 9 and C) of the transect. Mean Chl-*a* values in the upper 150 m layer were very low, 0.1–0.2 µg L^{-1} except at the two NW stations where they were slightly higher (St. 25, 27, Table 1). Below we refer to E and W basins, based on the simple geographical criterion employed by Longhurst (1998). Based on this division W and E stations are considered from 27 to 19 and from 13 to C, respectively. St. 17 and 15, situated in the Straight of Sicily are not included in the comparisons E-W, but these stations are included in the overall correlations between biological variables.

Among the parameters studied virus like particles (VLP) showed the highest variability as seen in the comparison of integrated abundances (Table 2). Volumetric values varied from 0.15 to 12.7×10^6 VLP ml^{-1} (Table 1). Mean VLP in the upper 150 m layer was on the order of low 10^6 ml^{-1} (Fig. 2a, Table 1). VLP was relatable to Chl-*a* concentration (n=116, $r^2 = 0.293$, p<0.0001) but a tighter relationship existed between VLP and heterotrophic bacterial abundances (HBA) (n=116, r^2=0.505, p<0.0001). The mean VLP/HBA ratio was highly variable and ranged from 3 to 96. HBA concentrations were on the order of 10^5 cells ml^{-1} (0.1 to 8.63×10^5 cells ml^{-1}, Table 1) and were clearly higher in the W than in the E basin (Fig. 2b). However, overall HBA was the parameter that showed the least variation in terms of integrated biomass along the transect (Table 2). A similar pattern was evident for bacterial production (BP) with lower volumetric values in the E and higher in the W (Fig. 2c, Table 1). Integrated values ranged from 24 to 74 mg C m^{-2} d^{-1} (Table 2).

Heterotrophic nanoflagellates (HNF, Fig. 2c) were dominated by small cells of mean equivalent spherical diameter of 2.46 µm and total abundances in the upper 150 m

from a few hundreds to a few thousands cells per ml (0.42–4.65×10^3 cells ml^{-1}). A significant log-log relationship was found between HBA and HNF abundances (n=153, r^2=0.289, p<0.0001).

Ciliates generally showed low abundances and in particular at the far eastern stations (Table 1, Fig. 2d). Highest ciliate abundances were recorded at the DCM level or just above it. The log-log linear regression between Chl-*a* concentration (µg L^{-1}) and ciliate abundance (cell L^{-1}) in the upper 150 m was highly significant (n=111, r^2=0.472, p<0.0001). However this relationship was tighter in the W (n=31, r^2=0.504, p<0.0001) than in the east E (n=72, r^2=0.215 p<0.001). The slopes of the regressions were not significantly different (t_{value}=0.41; ddl=101). Planktonic ciliates were dominated by the aloricate naked forms with tintinnids being abundant only at St. 25 just below the DCM (Fig. 2e, 75 m, 1164 cells L^{-1}, Fig. 2d). Mixotrophs, as a portion of ciliate biomass, varied from 13 to 77% (mean ± sd, 37 ± 14%). An exceptionally high contribution in terms of biomass of mixotrophs (90%) was recorded at St. 21 at the DCM level (Fig. 2d, Table 1). Log-transformed data of ciliate abundance and Chl-*a* concentration indicated a tight relationship between tintinnids and Chl-*a* (n=111, r^2=0.496, p<0.0001) followed by heterotrophic ciliates (n=111, r^2=0.455 p<0.0001) and a weaker relationship between mixotrophs and Chl-*a* (n=111, r^2= 0.201 p<0.0001).

3.2 Comparing stocks in and outside the 3 anticyclonic eddies

Sites A, B and C were located in the centre of 3 distinct anticyclonic eddies across the trophic gradient. At site A the bottom depth was 2800 m, the anticyclonic eddy was detectable down to 800 m and the core depth of the eddy was 100–250 m (Fig. 3a). A key feature characterizing site A was smooth phosphate and nitrate profiles contrasting with the sharp nutriclines observed in the neighbouring St. 21 outside of the eddy (Fig. 4a,b). All the heterotrophic parameters recorded showed lower values and the depth profiles were smoother inside the eddy than outside (Fig. 4a–f). Mean BP was about 2 fold lower inside the eddy (Table 1) and the BP profile was clearly smoother

inside the eddy than outside where it showed several irregularities (Fig. 4a,b). HBA and VLP showed very similar trends within and outside the eddy but with concentrations higher outside the eddy (Fig. 4c,d). HNF profiles were similar inside and outside the eddy and they did not show any particular trend with either HBA or VLP (Fig. 4c,d). Finally, the ciliates showed maximal abundance just above the DCM both within and outside the eddy but with ×3 more ciliates outside the eddy (Fig. 4e,f). Interestingly, outside the eddy at St. 21 mixotrophic ciliates were a more important component of the ciliate community, approximately 33% of total integrated biomass, compared to 18% of the eddy community.

At site B the bottom depth was 3200 m, the anticyclonic eddy was very deep extending down to 1500 m and the core depth of the eddy was 200–600 m (Fig. 3b). The same general pattern seen at site A was found for the site B: Flat nutrient profiles, with a deep nutricline, contrasting with shallower ones at St. 13 outside of the eddy (Fig. 5a,b), and generally lower values and smoother profiles inside the eddy (Fig. 5a–f). It is worthy to note that the fluorescence profile varied little with depth in the eddy with a weak maximum just above 150 m, while outside the eddy the fluorescence profile showed pronounced maxima. The fluorescence maxima at St. 13 were associated with the presence of *Prochlorococcus* at 80 m (116×10^3 Proc ml^{-1}), while at 140 m the maximum of fucoxanthine was observed (0.05 µg L^{-1}) associated with the presence of *Prochlorococcus* and *Synechococcus* (19.3 and 2.5×10^3 ml^{-1}, respectively, Courties and Ras, BOUM data). Mean bacterial production was again about 2 fold lower inside the eddy (Table 1). HBA and VLP showed similar trends in particular inside the eddy (Fig. 5c,d). HBA showed a deep maximum at the DCM outside the eddy. HNF profiles were again quite similar in terms of trend and absolute values inside and outside the eddy (Fig. 5c,d). Finally, ciliates showed in both cases maximal abundance just above the DCM and were about ×2 more abundant at St. 13 compared to inside the eddy. With regard to species assemblages, the tintinnid ciliate community appeared distinct with 11 species detected in the eddy samples only 4 of which were found also at St. 13.

Site C was situated in the ultra-oligotrophic East Mediterranean above the mount Eratosthenes (900 m). The eddy was detectable down to the bottom and the core depth of the eddy was 150–400 m (Fig. 3c). An unexpected feature of this eddy was the presence of measurable phosphate in surface waters (Fig. 6a, b). The deep fluorescence maximum was clearly more marked in the eddy and was associated with the presence of diatoms (active biogenic Si – Crombet et al., 2010). In contrast to the eddies of site A and site B, the general characteristic was a similarity for all parameters – except viruses – in and outside of the eddy (St. 11, Fig. 6a–f). Viruses were more abundant and showed a remarkably similar trend with HBA inside the eddy. Ciliate were found at their lowest abundances at these far-east stations with no marked differences inside and outside the eddy (Fig. 6e, f). The eddy and St. 11 ciliate communities were also similar in terms of the relative contribution of mixotrophic forms (about 29% of total integrated biomass).

3.3 Biological fluxes in the 3 anticyclonic eddies

Particulate primary production (PPp) and oxygen fluxes were measured twice at each site (Table 3). At sites A and B the two PPp integrated values estimated were similar, with slightly higher values in site B (156 vs. 164 and 195 vs. 187 mg C m^{-2} d^{-1}, respectively), while they varied more at site C (137 vs. 191 mg C m^{-2} d^{-1}). Considering all volumetric measurements together, PPp was related to BP (n=60, r^2=0.66, p<0.0001) and this relationship was very strong at sites A and B (n=20, r^2=0.81 and r^2=0.88, p<0.0001respectively) and weaker at C (n=20 r^2=0.44, p<0.0001). Integrated GCP and DCR, ranged 28–75 mmol O_2 m^{-2} d^{-1} (mean ± sd, 54 ± 18) and 39–58 mmol O_2 m^{-2} d^{-1} (mean ± sd, 50 ± 8), respectively, in the centre of the 3 eddies (Fig. 7). Similar to PPp, GCP was more variable at site C (28 and 75 mmol O_2 m^{-2} d^{-1}). Gross production roughly balanced with respiration and net community production (NCP) fluxes were not different from zero (Fig. 7). BP was measured along 4 profiles at each site (once per day). Average 0–150 m integrated values were 36.4 ± 7.6,

35.6 ± 2.9 and 27.5 ± 3.3 mg C m^{-2} d^{-1} (mean ± sd) at the sites A, B and C, respectively, and were barely statistically different only between A and C (ANOVA, p=0.035)

4 Discussion

4.1 General and longitudinal features

Our first objective was to document the vertical and spatial distribution of the heterotrophic components of the microbial food web through a transect of 17 stations. Previous studies have described the W-E gradient in the MS but in terms of isolated components of the microbial food web (e.g., Dolan et al., 1999; Christaki et al., 2001; Pitta et al., 2001; Van Wambeke et al., 2002). Our study is the first, to our knowledge, to encompass all the major components of the microbial food web, from viruses to ciliates and the biological fluxes at 3 mesoscale anticyclonic eddies situated in each of the 3 Mediterranean basins. Overall, our observations concerning the longitudinal gradients were in agreement with the reported west to east trends of deepening of DCM and increasing oligotrophy in terms of biomass and production from W-E (reviewed in Siokou et al., 2010).

Among the very few previous studies of viruses in open Mediterranean waters, viral abundance reported varied between 0.8 and 16×10^6 VLP ml^{-1} (e.g Guixa-Boixereau et al., 1999; Weinbauer et al., 2003; Magagnini et al., 2007). Our estimates of viral abundance for the early summer ranged similarly (0.16–12×10^6 VLP ml^{-1}). We found a weak relationship between Chl-*a* and VLP compared to the tight correlation of the latter with HBA (cf. Sect. 3.1) implying that heterotrophic bacteria are the more probable virus hosts compared to phytoplankton. Interestingly, integrated profiles of VLP and HBA showed the highest and the lowest variability, respectively (Table 2). Indeed volumetric VLP/HBA ratio varied over a wide range (3 to 96) suggesting that viral abundance may vary over short times reflecting different phases of infection and release of host cells. HNF abundance, similar to other stocks measured in this study, was about

×2 higher in the west, but this parameter showed overall relatively low variability (30%, Table 2). All the values of the log-log plot of HNF and HBA fell above the 'Mean Realized Abundance' (MRA) for marine environments suggesting that HNF are resource, or bottom-up controlled by heterotrophic bacteria (*sensu* Gasol, 1994, figure not shown). This view is also supported by a significant slope of this relationship (n=153, r^2=0.29, p<0.0001). In a recent review of Mediterranean plankton (Siokou et al., 2010), a similar log-log relation between HNF and bacteria was found, with most of the values falling above MRA. The relative stability of bacterial numbers also suggests that bacterial production was tightly matched by bacterial mortality.

Ciliate abundance at different stations displayed high variability with roughly a 2-fold decrease overall for ciliate standing stock from W to E, in agreement with previous studies (Dolan et al. 1999; Pitta et al., 2001; Dolan et al. 2002). Ciliates in our study showed a significant relationship with Chl-*a* and their maximum abundances were related to the DCM (Dolan and Marrasé, 1995; Dolan et al. 1999). Compiled data from different studies in the MS have shown that this relationship may be stronger in the W than in the E basins (Siokou et al., 2010), this same pattern was found in our study. Mixotroph contribution to ciliate biomass was important and within the range reported in the few other existing studies of open Mediterrean waters (Pérez et al., 1997; Dolan et al., 1999; Pitta et al., 2001). The mixotrophic/autotrophic ciliate *Myrionecta rubra* was pooled with taxa of mixotrophic ciliates (*Tontonia* spp., *Laboea strobila*, *Strombidium acutum, Strombidium capitatum and Strombidium conicum*). The use of Lugol's fixative precluded identification of mixotrophic ciliates without distinctive gross morphology (i.e., certain small *Strombidium* species), the heterotrophic group likely contained some mixotrophs and thus our mixotroph numbers can be underestimated. However, since the mixotrophs considered in our study are the larger forms according to Dolan et al. (1999) and Karayanni et al. (2004), they represent most of the mixotrophic biomass. Dolan et al. (1999) and Pitta et al. (2001) have reported a more important contribution of mixotrophs in the E compared to the W basin. This pattern was not clear during our study since the contribution of mixotrophs was slightly – but

not significantly – lower in the W (33 ± 19% and 39 ± 15% in W and E, respectively). Overall, mixotrophs showed a high variability in their contribution in total ciliate biomass (Table 2) and the mixotrophs *S. acutum* and *S. capitatum* dominated ciliate biomass at St. 25 at the DCM level (Fig. 2e, 90% of ciliate biomass). In a recent study in the Western Mediterranean Sea, mixotrophs were found to be efficient grazers of nanophytoplankton forming dense populations related to high Chl-*a* concentrations (Christaki et al., 2009). Tintinnids are also known to form patchy distributions related to their food resources (e.g., Alder and Boltovskoy 1991; Christaki et al., 2008). Accordingly, the unique high tintinnid abundance recorded was in the W at the station and depth where the highest concentration of Chl-*a* during BOUM cruise was measured (St. 25, Table 1, Fig. 2f).

4.2 Stocks and biological fluxes in the 3 anticyclonic eddies

Our second objective was to examine the microbial food webs within anticyclonic mesoscale eddies. Our hypothesis was that the impact of eddies would be recognizable within the broader W-E gradient of oligotrophy. The 3 eddies were indeed associated with the lowest values for different metrics of the heterotrophic compartments of the microbial food web. This was particularly pronounced for ciliates (both heterotrophs and mixotrophs) which are the link between microbial food web and the higher trophic levels. A question that arises is: Is the oligotrophy gradient detectable among eddies? The W-E gradient, although attenuated, was clearly recognizable among the 3 eddies and except for virus in site C, all stocks are higher at the stations outside the eddies (Fig. 8). This was particularly pronounced for virus, heterotrophic bacteria and HNF, and less pronounced for ciliates. Interestingly, among ciliates, mixotrophs did not show any recognizable pattern in terms of stocks from sites A to C (Fig. 8). Considering however their contribution to ciliate biomass, it was larger at sites B and C (43% and 29%, respectively) and lower at site A (18%).

Overall, a W-E gradient among the eddies was generally recognizable in terms of heterotrophic biomass values but not in terms of production. Integrated BP was very similar at the 3 eddies (33.5 ± 6 mg C m^{-2} d^{-1}). This mean value in the eddies

matches the mean integrated BP of the deep, open sea stations of the E basin (39 ± 15 mg C m^{-2} d^{-1}) and was clearly lower than the mean integrated BP of the deep, open sea stations of the W basin (61 ± 7 mg C m^{-2} d^{-1}, Van Wambeke et al., 2010). The integrated bacterial production values obtained in the 2 basins were of similar order to the ones reported before in open MS waters (e.g., Pedros-Alio et al., 1999; Christaki et al., 2001; Van Wambeke et al., 2002, 2004).

Particulate primary production during BOUM cruise, using 24h-long in situ incubations from dawn to dawn, was measured only in the three eddies. Means of integrated PPp values were higher at site B (~190 mg C m^{-2} d^{-1}) and about 15% lower at sites A and C (~160 mg C m^{-2} d^{-1}). These values are situated at the lower range of PPp values reported previously in open MS waters (e.g; Moutin and Raimbault 2002) using the same JGOFS protocol. The integrated BP/PPp ration was on average 0.17 ± 0.04 over the 3 sites and corresponded to the ratio generally obtained in oligotrophic environments (Ducklow, 2000) It is probable that the coupling between both processes is high as shown by the strong positive relationship between volumetric BP and PPp data (e.g., Turley et al., 2000).

Unfortunately, little information is available on percentages of extracellular release of photosynthate in the Mediterranean Sea, data which is needed to compute total primary production, PP_{total} (excluding heterotrophic respiration and photorespiration). During the BOUM cruise, the percentage of PER was determined 3 times in each eddy (Lopez-Sandoval et al., 2010). PER was significantly lower in site A compared to C (ANOVA test, p=0.01), with means of 29 ± 1, 35 ± 3 and 39 ± 5 at sites A, B and C, respectively. Largest variability of PER, from one day to another at one given eddy, was found for the site C. This relatively high variability was also seen for PPp and GCP, and for this reason for computing PP_{total} we used each profile's values instead of means (Table 3).

The relatively high PPp at station C is rather unexpected in the sense that it diverges from the established W-E decreasing productivity gradient as it is equal to, or even higher than (at the second day), values with stations B and A. Moreover, compared to

previous estimates (May 2002) in the warm core Cyprus eddy during the CYCLOPS experiment (Psarra et al., 2005), Chl-*a* and primary production values reported here are 2-fold higher. If we compare station C to the western station A, there are several interesting differences. The elevated integrated PPp values at station C may be attributed to a deep maxima recorded at 80–100 m depth, since values in the 0–80 m layer were lower than those in stations A and B (data not shown). Interestingly, these deep PPp and Chl-*a* maxima are mostly associated with an N/P<10 and the presence of diatoms and prymnesiophytes whereas the respective maxima of Chl-*a* at station A (90 m) are associated with an N/P>25 and the presence of cyanobacteria and prymnesiophytes (Crombet et al., this issue). Interpretation of this peculiar character of station C is not straightforward. A plausible explanation might be the presence of relatively elevated PO_4 values in the entire surface layer (0–150 m), generally 4 times higher that those at stations A and B, despite a deeper phosphacline at station C. The origin of the higher PO_4 concentrations at station C remains obscure. However, we might argue that the elevated phytoplankton biomass and production observed at station C were related to those higher PO_4 concentrations, at an optimum depth (80–100 m) where there were enough NO_3 and light to sustain productivity and growth. Most probably, the bottom topography and vertical structure of the eddy at station C (warmer and shallower) may have played a critical role in structuring the above mentioned characteristics. Thus, based on these observations, we might argue that mesoscale activity alone is not always sufficient to interpret the microbial food web dynamics within the Mediterranean eddies, and consideration of the complexities engendered by particular geographic characteristics and external inputs require consideration.

Some data from previous reports exists on the contribution of bacterial respiration (BR) to Dark Community Respiration (DCR) in the Mediterranean Sea. In the NW Mediterranean Sea, at the open water Dyfamed site, the mean ratio BR/DCR over an annual cycle was 65% (Lemée et al., 2002), and at a coastal site, an average value of 52% (range 41 to 85%) was recorded (Navarro et al., 2004). BR ranged from 0 to 36.4 mmol O_2 L^{-1} d^{-1} (Lemée et al., 2002; Navarro et al., 2004). BR was not

measured during BOUM cruise. However, assuming that BR accounted for 50% of DCR, then the Bacterial Growth Efficiency (BGE=BP/(BP+BR)) would be on average 11 ± 2% in the 3 eddies (based on integrated data of Table 3). Generally BGE tends to be low in oligotrophic systems, perhaps because most of the DOC pool is recalcitrant and inorganic nutrients are scarce (del Giorgio et al., 1997). Indeed, in the Almeria-Oran geostrophic front and adjacent Mediterranean waters BGE was estimated to be 7% (Sempéré et al., 2003) and lower values (2.6 ± 0.1%) were obtained in the NW-Mediterranean through a coastal offshore gradient (Moran et al., 2002). Therefore, a BGE estimate of 11% which may be high, argues that BR represented at least 50% of DCR.

Low oxygen fluxes are particularly difficult to estimate with accuracy. With the exception of a seasonal study at a fixed station in the Ligurian Sea (Lemée et al., 2002) and a late-spring early summer cruise in the open MS by Regaudie-de Gioux et al. (2009) very few data on planktonic O_2 metabolism exists in the Mediterranean and they are mostly restricted to coastal/frontal areas of the Western Mediterranean (Lefèvre et al., 1997, Van Wambeke et al., 2004). Our integrated GCP (28–75 mmol O_2 m^{-2} d^{-1}) and DCR (39–58 mmol O_2 m^{-2} d^{-1}) values fell within the range of previously recorded values except the ones reported by Regaudie-de Gioux et al. (2009), which were higher (mean GCP 118–196 mmol O_2 m^{-2} d^{-1}).

Oxygen production in the upper 15 m of the surface is roughly balanced by respiration. The balance between GCP and DCR respiration in oceanic system determines whether the biological pump acts as a net source or sink of carbon (Williams, 1993). NCP varies with geographical, temporal, seasonal scales and is also strongly influenced by mesoscale variability (del Giorgio and Duarte 2002; Maixandeau et al., 2005). It has been shown also to vary rapidly over a MS transect (Regaudie-de Gioux et al., 2009). During our study, the 3 eddies showed equilibrium between GCP and DCR, suggesting a NCP close to zero (4 ± 15 mmol O_2 m^{-2} d^{-1}) (Fig. 7). Assuming then that heterotrophic bacterial respiration was 50% of DCR (see below), then PP_{total} was sufficient to sustain bacterial carbon demand at the sites B and C where fluxes were roughly

equal (Table 3) while this was not the case at the site A (ratio BCD/PP_{total} 1.3–1.4). The net heterotrophy, although not statistically significant at site A, is in accordance with the BCD/PP_{total} ratio slightly higher than 1.

5 Conclusions

We present, for the first time, data on all the major components of the heterotrophic part of the microbial food web across the MS. The large-scale pattern revealed is overall in agreement with the well established longitudinal gradient of increasing oligotrophy in terms of biomass and production from the W to the E. However, we also showed that mesoscale features such as the 3 anticyclonic eddies studied during the cruise display particular microbial dynamics. Limited data on ciliate community composition suggested that eddy microbial communities differed from those in adjacent stations outside the eddies. During our study the 3 eddies showed equilibrium between GCP and DCR, moreover, the W-E gradient was recognizable in terms of heterotrophic biomass but not in terms of production. Our estimates, based on the assumption that bacteria are responsible for 50% of DCR, indicated that autotrophic production alone was barely sufficient to supply the bacterial carbon demand at the eddies (B, C) situated in the central and E basins and insufficient at the eddy (A) situated in the W, suggesting that phytoplankton production and that of heterotrophic prokaryotes was decoupled. Our results, documenting variability in microbial processes and community composition, suggest that spatial heterogeneity in the form of mesoscale features such as eddies likely require incorporation into predictive models of ecosystem functioning.

Acknowledgements. This is a contribution of the BOUM (Biogeochemistry from the Oligotrophic to the Ultraoligotrophic Mediterranean) experiment (http://www.com.univ-mrs.fr/BOUM) of the French national LEFE-CYBER program, the European IP SESAME and the international IMBER project. The BOUM experiment was coordinated by the Institut des Sciences de l'Univers (INSU) and managed by the Centre National de la Recherche Scientifique (CNRS). We also thank Josephine Ras for pigment analysis.

The publication of this article is financed by CNRS-INSU.

References

Adler, V. A. and Boltovskoy, D.: Microplanktonic distributional patterns west of the Antarctic Peninsula, with special emphasis on the tintinnids, Polar Biol., 11, 103–112, 1991.

Brussaard, C. P. D.: Optimization of procedures for counting viruses by flow cytometry, Appl. Environ. Microb., 70, 1506–1513, 2004.

Christaki, U., Giannakourou, A., Van Wambeke, F., and Gregori, G.: Nanoflagellate predation on auto- and heterotrophic picoplankton in the oligotrophic Mediterranean Sea, J. Plankton Res., 23, 1297–1310, 2001.

Christaki, U., Obernosterer, I., Van Wambeke, F., Veldhuis, M., Garcia, N., and Catala, P.: Microbial food web structure in a naturally iron fertilized area in the Southern Ocean (Kerguelen Plateau), Deep-Sea Res. Pt. II, 55, 706–719, doi:10.101/j.dsr2.2007/12.009, 2008.

Christaki, U., Courties, C. Joux, F., Jeffrey, W. H., Neveux, J., and Naudin, J. J.: Community structure and trophic role of ciliates and heterotrophic nanoflagellates in Rhone River diluted mesoscale structures (NW Mediterranean Sea), Aquat. Microb. Ecol., 57, 263–277, 2009.

Crombet, Y., Leblanc, K., Quéguiner, B., Moutin, T., Rimmelin, P., Ras, J., Claustre, H., Leblond, N., Oriol, L., and Pujo-Pay, M.: Deep silicon maxima in the stratified oligotrophic Mediterranean Sea, Biogeosciences Discuss., 7, 6789–6846, doi:10.5194/bgd-7-6789-2010, 2010.

Del Giorgio, P., Cole, J., and Cimbleris, A.: Respiration rates in bacteria exceed phytoplankton production in unproductive aquatic systems, Nature, 385, 148–151, 1997.

Del Giorgio, P. A. and Duarte, C. M.: Respiration in the open ocean, Nature, 420, 379–384, 2002.

Dolan, J. R. and Marrasé, C.: Planktonic ciliate distribution relative to a deep chlorophyll maximum: Catalan Sea, N. W. Mediterranean, Deep-Sea Res. Pt. I, 42, 1965–1987, 1995.

Dolan, J. R., Claustre, H., Carlotti, F., Plouvenez, S., and Moutin, T.: Microzooplankton diversity:

relationships of tintinnid ciliates with resources, competitors and predators from the Atlantic Coast of Morocco to the Eastern Mediterranean, Deep-Sea Res. Pt. I, 49, 1217–1232, 2002.

Dolan, J., Vidussi, F., and Claustre, H.: Planktonic ciliates in the Mediterranean Sea: longitudinal trends, Deep-Sea Res. Pt. I, 46, 2025–2039, 1999.

Ducklow, H.: Bacterial production and biomass in the ocean, in: Microbial Ecology of the Oceans, edited by: Kirchman, D. L., Wiley-Liss, Inc, New York, 85–120, 2000.

Dugdale, R. C. and Wilkerson, F. P.: Nutrient sources and primary production in the Eastern Mediterranean, Oceanol. Acta, Special Issue, 179–184, 1988.

Fukuda, R., Ogawa, H., Nagata, T., and Koike, I.: Direct determination of carbon and nitrogen contents of natural bacterial assemblages in marine environments, Appl. Environ. Microb., 64, 3352–3358, 1998.

Gasol, J. M.: A framework for the assessment of top-down vs. bottom-up control of heterotrophic nanoflagellates abundance, Mar. Ecol.-Prog. Ser., 113, 291–300, 1994.

Guixa-Boixereu, N., Vaqué , D., Gasol, J., and Pedros-Alio, C.: Distribution of viruses and their potential effect on bacterioplankton in an oligotrophic marine system, Aquat. Microb. Ecol., 19, 205–213, 1999.

Ignatiades, L., Gotsis-Skretas, O., Pagou, K., and Krasakopoulou, E.: Diversification of phytoplankton community structure and related parameters along a large-scale longitudinal east-west transect of the Mediterranean Sea, J. Plankton Res., 31, 411–428, 2009.

Karayanni, H., Christaki, U., Van Wambeke, F., and Dalby, A.: Evaluation of double formol – lugol fixation in assessing number and biomass of oligotrich heterotrophs, mixotrophs and tintinnids, An example of estimations at mesoscale in NE Atlantic, J. Microbiol. Meth., 54, 349–358, 2004.

Krom, M. D., Kress, N., Brenner, S., and Gordon, L.: Phosphorous limitation of primary productivity in the Eastern Mediterranean Sea, Limnol. Oceanogr., 36, 424–432, 1991.

Laws, E. A. : Photosynthetic quotients, new production and net community production in the open ocean. Deep-Sea Res., 38(1), 143–167, 1991.

Lefèvre, D., Minas, H. J., Minas, M., Robinson, C., Williams, P. J. Le B., and Woodward, E. M. S.: Review of gross community production, primary production, net community production and dark community respiration in the Gulf of Lions, Deep-Sea Res. Pt. II, 44, 801–832, 1997.

Lefèvre, D., Guigue, C., and Obernosterer, I.: The metabolic balance at two contrasting sites in the Southern Ocean: the iron-fertilized Kerguelen area and HNLC waters, Deep-Sea Res. Pt. II, 55, 766–776, 2008.

Lemée, R., Rochelle-Newall, E., Van Wambeke, F., Pizay, M., Rinaldi, P., and Gattuso, J.: Seasonal variation of bacterial production, respiration and growth efficiency in the open NW Mediterranean Sea, Aquat. Microb. Ecol., 29, 227–237, 2002.

López-Sandoval, D. C., Fernández, A., and Marañón, E.: Dissolved and particulate primary production along a longitudinal gradient in the Mediterranean Sea, Biogeosciences Discuss., 7, 8591–8617, doi:10.5194/bgd-7-8591-2010, 2010.

Lunghurst, A.: Ecological Geography of the Sea, Academic Press, San Diego, 398 pp., ISBN O-12-455558-6, 1998.

Lynn, D. H.: The Ciliated Protozoa: Characterization, Classification,and Guide to the Literature, 3rd edn., Springer, Berlin, 606 pp., 2008.

Magagnini, M., Corinaldesi, C., Monticelli, L. S., De Domenico, E., and Danovaro, R.: Viral abundance and distribution in mesopelagic and bathypelagic waters of the Mediterranean bacteria in an oligotrophic sea – the Mediterranean and biogeochemical implications, Mar. Ecol.-Prog. Ser., 193, 11–18, 2000.

Maixandeau, A., Lefèvre, D., Karayanni, H., Christaki, U., Van Wambeke, F., Thyssen, M., Denis, M., Fernadez, C., Uitz, J., Leblanc, K., and Quéguiner, B.: Respiration in relation to microbial food web structure in Northeastern Atlantic Ocean, J. Geophys. Res., 110, C07S17, doi:10.1029/2004JC002694, 2005.

Marie, D., Brussaard, C. P. D., Partensky, F., and Vaulot, D.: Flow cytometric analysis of phytoplankton, bacteria and viruses, in: Current Protocols in Cytometry, edited by: Robinson J., 1–15, John Wiley & Sons, Inc, New York, 1999.

Moran, X. A. G., Estrada, M., Gasol, J. M., and Pedros-Alio, C.: Dissolved primary production and the strength of phytoplankton–bacterioplankton coupling in contrasting marine regions, Microb. Ecol., 44, 217–223, 2002.

Moutin, T., Raimbault, P., and Poggiale, J.-C.: Primary production in surface waters of the Western Mediterranean sea, Calculation of daily production, CR Acad. Sci. III-Vie., 322, 651–659, 1999.

Moutin, T. and Raimbault, P.: Primary production, carbon export and nutrients availability in Western and Eastern Mediterranean Sea in early summer 1996 (MINOS cruise), J. Marine Syst., 33, 273–288, 2002.

Navarro, N., Agusti, S., and Duarte, C. M.: Plankton metabolism and dissolved organic carbon use in the Bay of Palma, NW Mediterranean Sea, Limnol. Oceanogr., 37, 47–54, 2004.

Pedros-Alio, C., Calderon-Paz, J., Guixa-Boixereu, N., Estrada, M., and Gasol, J.: Bacteri-

oplankton and phytoplankton biomass and production during summer stratification in the Northwestern Mediterranean Sea, Deep-Sea Res. Pt. I, 46, 985–1019, 1999.

Peréz, M., Dolan, J., and Fukai, E.: Planktonic oligotrich ciliates in the NW Mediterranean: growth rates and consumption by copepods, Mar. Ecol.-Prog. Ser., 155, 89–101,1997.

Pitta, P., Giannakourou, A., and Christaki, U.: Planktonic ciliates in the oligotrophic Mediterranean Sea: longitudinal trends of standing stocks, distributions and analysis of food vacuole contents, Aquat. Microb. Ecol., 24, 297–311, 2001.

Psarra, S., Zohary, T., Krom, M. D., Mantoura, R. F. C., Polychronaki, T., Stambler, N., Tanaka, T., Tselepides, A., and Thingstad, F. T.: Phytoplankton response to a Lagrangian phosphate addition in the Levantine Sea (Eastern Mediterranean), Deep-Sea Res. Pt. II, 52, 2944–2960, 2005.

Pujo-Pay, M., Conan, P., Oriol, L., Cornet-Barthaux, V., Falco, C., Ghiglione, J.-F., Goyet, C., Moutin, T., and Prieur, L.: Integrated survey of elemental stoichiometry (C, N, P) from the Western to Eastern Mediterranean Sea, Biogeosciences Discuss., 7, 7315–7358, doi:10.5194/bgd-7-7315-2010, 2010.

Putt, M. and Stoecker, D. K.: An experimentally determined carbon: volume ratio for marine "oligotrichous" ciliates from estuarine and coastal waters, Limnol. Oceanogr., 34, 1097–1103, 1989.

Ras, J., Claustre, H., and Uitz, J.: Spatial variability of phytoplankton pigment distributions in the Subtropical South Pacific Ocean: comparison between in situ and predicted data, Biogeosciences, 5, 353–369, doi:10.5194/bg-5-353-2008, 2008.

Regaudie-de-Gioux, A., Vaquer-Sunyer, R., and Duarte, C. M.: Patterns in planktonic metabolism in the Mediterranean Sea, Biogeosciences, 6, 3081–3089, doi:10.5194/bg-6-3081-2009, 2009.

Schlitzer, R.: Ocean Data View 4, http://odv.awi.de, 2009.

Sempéré, R., Dafner, E., Van Wambeke, F., Lefèvre, D., Magen, C., Allère, S., and Bruyant, F.: Almeria-Oran front in the Mediterranean Sea: implications for carbon cycling in the western basin, J. Geophys. Res., 108, 3361, doi:10.1029/2002JC001475, 2003.

Siokou-Frangou, I., Christaki, U., Mazzocchi, M. G., Montresor, M., Ribera d'Alcalá, M., Vaqué, D., and Zingone, A.: Plankton in the open Mediterranean Sea: a review, Biogeosciences, 7, 1543–1586, doi:10.5194/bg-7-1543-2010, 2010.

Smith, D. C. and Azam, F.: A simple, economical method for measuring bacterial protein synthesis rates in sea water using 3H-Leucine, Marine Microb. Food Webs, 6, 107–114, 1992.

Thingstad, F. T., Krom, M. D., Mantoura, R., Flaten, G., Groom, S., Herut, B., Kress, N., Law, C., Pasternak, A., Pitta, P., Psarra, S., Rassoulzadegan, F., Tanaka, T., Tselepides, A., Wassmann, P., Woodward, E., Wexels, Riser, C., Zodiatis, G., and Zohary, T.: Nature of phosphorus limitation in the ultraoligotrophic Eastern Mediterranean, Science, 309, 1068–1071, 2005.

Turley, C., Bianchi, M., Christaki, U., Conan, P., Harris, J. R. W., Psarra, S., Ruddy, G., Stutt, E., Tselepides, A., and Van Wambeke, F.: Relationship between primary producers and bacteria in an oligotrophic sea-the Mediterranean and biogeochemical implications, Mar. Ecol.-Prog. Ser., 193, 11–18, 2000.

Tréguer, P. and Le Corre, P.: Manuel d'analyses des sels nutritifs dans l'eau de mer, Laboratoire d'Océanographie Chimique, Université de Bretagne Occidentale, Brest, 110 pp., 1975.

Van Wambeke, F., Christaki, U., Giannakourou, A., Moutin, T., and Souvemerzoglou, K.: Longitudinal and vertical trends of bacterial limitation by phosphorus and carbon in the Mediterranean Sea, Microb. Ecol., 43, 119–133, 2002.

Van Wambeke, F., Lefèvre, D., Prieur, L., Sempéré, R., Bianchi, M., Oubelkheir, K., and Bruyant, F.: Distribution of microbial biomass, production, respiration, dissolved organic carbonand factors controlling bacterial production across a geostrophic front (Almeria-Oran, SW Mediterranean Sea), Mar. Ecol.-Prog. Ser., 269, 1–15, 2004.

Van Wambeke, F., Catala, P., and Lebaron, P.: Relationships between cytometric characteristics of high and low nucleic-acid bacterioplankton cells, bacterial production and environmental parameters along a longitudinal gradient across the Mediterranean Sea, Biogeosciences Discuss., 7, 8245–8279, doi:10.5194/bgd-7-8245-2010, 2010.

Videau, C., Sournia, A., Prieur, L., and Fiala, M.: Phytoplankton and primary production characteristics at selected sites in the geostrophic Almeria-Oran front system (SW Mediterranean Sea), J. Marine Syst., 5, 235–250, 1994.

Weinbauer, M., Brettar, I., and Höfle, M.: Lysogeny and virus induced mortality of bacterioplankton in surface, deep, and anoxic marine waters, Limnol. Oceanogr., 48, 1457–1465, 2003.

Williams, P. J. L. and Jenkinson, N. W.: A transportable microprocessor-controlled precise Winkler titration suitable for field station and shipboard use, Limnol. Oceanogr., 27, 576–584, 1982.

Williams, P. J. Le B.: Chemical and tracer methods of measuring plankton production, ICES Mar. Sc., 197, 20–36, 1993.

Table 1. Physico-chemical and biological (range and mean) of 17 sampling station in the upper 150 m (except St. 17 and St. 27, 0–100 m) in the Mediterranean in June–July 2008. DCM: deep Chlorophyll maximum depth, VLP: virus particles, HBA: heterotrophic bacteria, HNF: heterotrophic nanoflagellates, Cil: ciliates, BP: bacterial production, nd: no data. A, B, and C stations representing selected anticyclonic eddies are depicted in bold letters.

Station W→E	Date (2008)	Cast CTD	Longitude N	Latitude E	Chl-*a* ($\mu g\,L^{-1}$)	DCM (m)	VLP ($10^6\,ml^{-1}$)	HBA ($10^5\,ml^{-1}$)	HNF ($10^3\,ml^{-1}$)	Cil ($10\,L^{-1}$)	BP ($ng\,C\,L^{-1}\,h^{-1}$)
27	18 Jul	199	43° 20,967′	4° 93,050′	0.06–0.37 0.24	30	2.92–7.92 5.88	3.63–8.63 5.78	1.03–3.26 2.15	nd	nd
25	18 Jul	191	41° 99,633′	4° 98,550′	0.004–1.7 0.32	50	1.39–12.66 5.38	0.19–1.02 0.56	1.44–4.65 2.65	5–157 45	1.3–40.7 18.2
24	18 Jul	189	41° 08,850′	5° 05,567′	0.04–0.66 0.19	70	2.05–8.26 5.28	0.22–0.93 0.66	1.79–3.15 2.54	13–61 38	2.2–34.9 21.2
A	**14–16 Jul**	**161**	**39° 10,617′**	**5° 30,967′**	**0.01–0.26 0.1**	**90**	**1.38–5.91 3.58**	**0.23–0.71 0.44**	**1.27–4.32 2.41**	**12–38 22**	**1.8–14.2 7.8**
21	11 Jul	129	38° 63,750′	7° 91,783′	0.01–0.38 0.13	85	1.58—5.93 4.42	0.21–0.71 0.53	1.66–2.82 2.40	21–128 70	4.2–31.6 17.7
19	10 Jul	126	38° 10,233′	10° 22,550′	0.01–0.52 0.16	70	1.23–3.84 2.56	0.17–0.71 0.50	1.55–3.46 2.46	nd	1.7–29.6 18.9
17	9 Jul	123	37° 16,750′	11° 99,817′	0.06–0.26 0.13	80	2.66–4.15 3.47	0.52–0.77 0.65	1.31–3.60 2.35	27–8658 58	1.7–38.9 28.5
15	8 Jul	120	35° 66,833′	14° 10,017′	0.04–0.3 0.13	100	0.82–3.46 2.16	0.19–0.70 0.54	1.51–2.51 2.03	nd	6.5–43.9 20.9
13	8 Jul	117	34° 88,500′	16° 69,850′	0.04–0.27 0.14	93	1.00–2.80 1.99	0.35–0.68 0.53	1.07–2.19 1.52	22–58 41	5.6–35.9 19.9
B	**4–7 Jul**	**88**	**34° 13,350′**	**18° 45,550′**	**0.04–0.21 0.11**	**120**	**0.38–2.97 1.53**	**0.15–0.49 0.36**	**0.79–2.35 1.35**	**17–32 22**	**2.0–17 9.2**
1	21 Jun	3	34° 33,050′	19° 81,867′	0.05–0.58 0.18	85	0.7–4.34 1.34	2.17–6.65 4.57	0.65–1.73 1.20	34–90 62	2.1–20.9 10.8
3	21 Jun	6	34° 18,517′	22° 16,100′	0.03–0.68 0.17	110	0.15–0.91 0.25	0.13–0.48 0.34	0.90–1.47 1.18	13–64 34	1.8–30.8 10.2
5	22 Jun	9	34° 04,600′	24° 49,733′	0.03–0.34 0.12	115	0.18–0.35 0.19	0.10–0.49 0.27	0.74–2.22 1.41	19–46 34	2.0–13.6 9.2
7	23 Jun	12	33° 90,317′	26° 83,533′	0.04–0.40 0.15	100	1.27–2.45 1.79	0.22–0.54 0.40	0.88–1.73 1.27	25–71 52	2.8–18.2 11.6
9	24 Jun	15	33° 76,250′	29° 17,583′	0.03–0.22 0.10	120	0.16–0.56 0.29	0.11–0.38 0.26	0.69–1.73 1.34	21–47 30	3.4–11.9 6.9
11	25 Jun	18	33° 58,283′	31° 93,000′	0.03–0.24 0.09	110	0.45–1.12 0.78	0.17–0.43 0.28	0.42–1.53 1.04	17–27 21	1.5–12.6 6.4
C	**27–29 Jun**	**44**	**33° 62,650′**	**32° 65,283′**	**0.03–0.40 0.16**	**120**	**0.96–2.48 1.27**	**0.13–0.46 0.29**	**0.67–1.52 1.04**	**8–28 19**	**2.9–14 8.4**

Table 2. Integrated values in the upper 150 m (except St. 17 and St. 27, 0–100 m) in the Mediterranean June–July 2008. VLP: virus particles, HBA: heterotrophic bacteria, HNF: heterotrophic nanoflagellates, Cil_{tot}: total ciliates, Cil_{mixo}: mixotrophic ciliates BP: bacterial production.

	VLP $\times 10^{13}\,m^{-2}$	HBA $\times 10^{12}\,m^{-2}$	HNF $\times 10^{10}\,m^{-2}$	Cil_{tot} $\times 10^{9}\,m^{-2}$	Cil_{mixo} $\times 10^{9}\,m^{-2}$	BP $mg\,C\,m^{-2}\,d^{-1}$
Minimum	3	39	14	27	8	24
Maximum	66	82	37	96	40	74
Mean ± sd	33 ± 20	61 ± 13	25 ± 8	54 ± 20	22 ± 11	44 ± 17
Coeff. variation	0.6	0.2	0.3	0.4	0.5	0.4

Table 3. Integrated values of: Bacterial Production (BP), Particulate Primary Production (PP_p) and Total Primary Production (PP_{total}), the first (A1, B1 and C1) and the third day (A3, B3 and C3) of site occupation. Integrated Dark Community Respiration in terms of carbon (DCR_{CO_2}) is estimated assuming respiratory quotient=0.8, and Bacterial Carbon Demand (BCD=BP+BR) assuming that bacterial respiration was responsible for 50% of the DCR.

	BP $mg\,C\,m^{-2}\,d^{-1}$	PP_p $mg\,C\,m^{-2}\,d^{-1}$	PP_{total} $mg\,C\,m^{-2}\,d^{-1}$	DCR_{CO_2} $mg\,C\,m^{-2}\,d^{-1}$	BCD $mg\,C\,m^{-2}\,d^{-1}$	BCD/PP_{total}
A1	24.6	156	224	525	287	1.3
A3	36.3	164	229	554	313	1.37
B1	32.7	195	306	430	248	0.81
B3	36.7	187	271	452	263	0.97
C1	26.5	137	206	373	213	1.03
C3	24.5	191	317	546	297	0.94

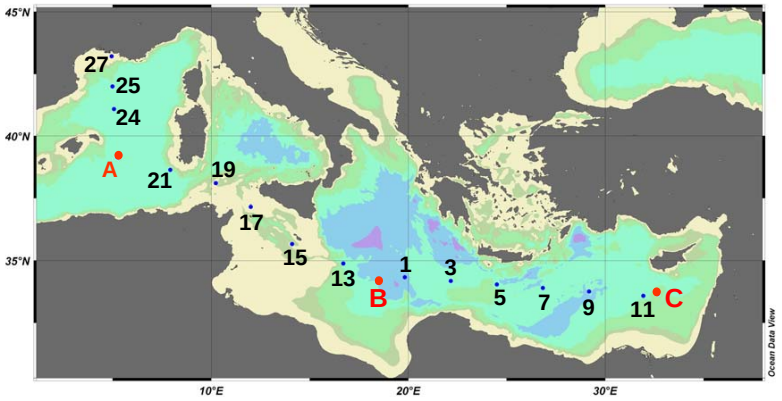

Fig. 1. Stations occupied for microbial metabolism and heterotrophic microplankton studies during the BOUM cruise (June–July, 2008). The sites A, B and C are situated in the center of 3 anticyclonic eddies.

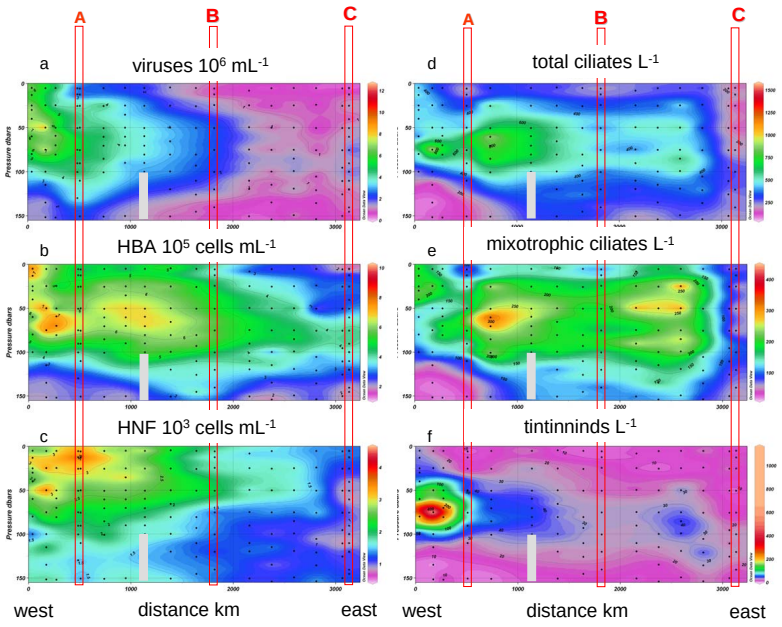

Fig. 2. Distribution of the abundance of virus **(a)**, heterotrophic bacteria **(b)**, heterotrophic nanoflagellates **(c)**, total ciliates **(d)**, mixotrophic ciliates **(e)** and tintinnids **(f)** in the upper 150 m along the MS transect. Interpolation between sampling points in contour plots was made with Ocean Data View program (VG gridding algorithm, Schlitzer, 2004).

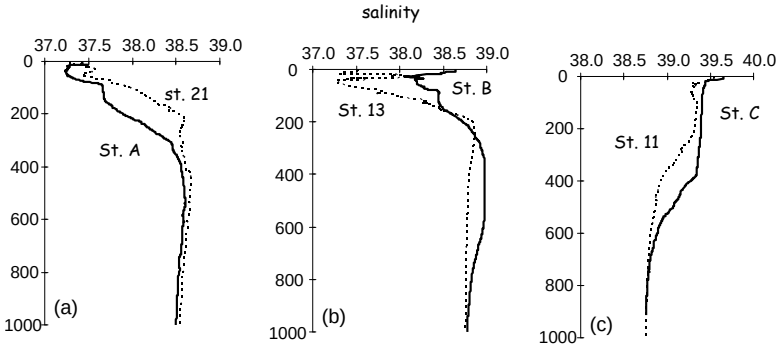

Fig. 3. Temperature and salinity profiles inside and outside of the 3 anticyclonic eddies, solid lines – inside the eddy, dotted lines – outside the eddy (cf. also Fig. 1).

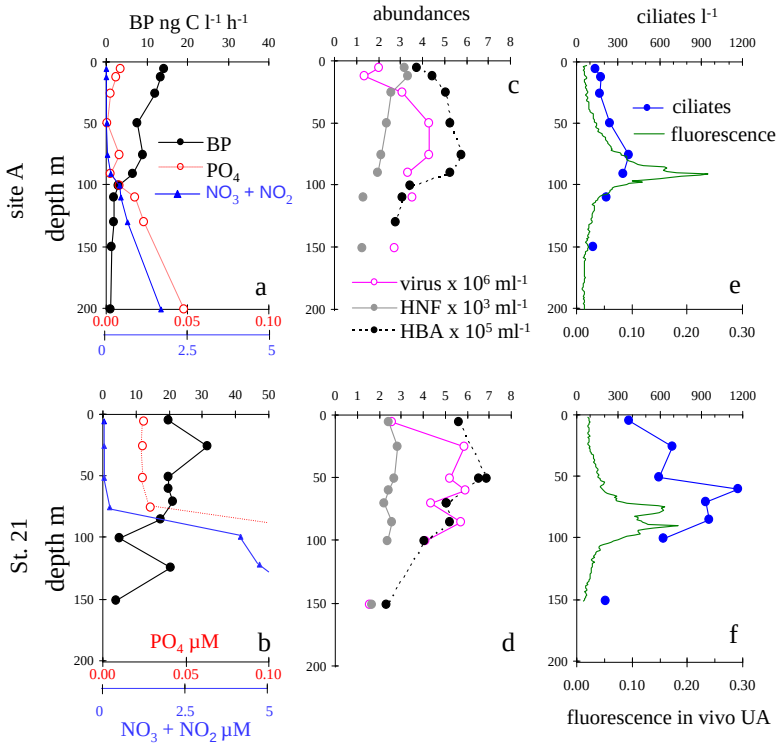

Fig. 4. Profiles of bacterial production (ng C l^{-1} h^{-1}), PO_4 and NO_2+NO_3 (µM) **(a, b)**, viral (VLP, 10^6 ml^{-1}), bacterial (HBA, 10^5 ml^{-1}) and heterotrophic nanoflagellate abundance (HNF, 10^3 ml^{-1}) **(c, d)**, ciliate abundance (l^{-1}) and in situ fluorescence **(e, f)** in the center of the eddy A (upper panel **a**, **c**, and **f**) and at St. 21 (lower panel **b**, **d** and **e**).

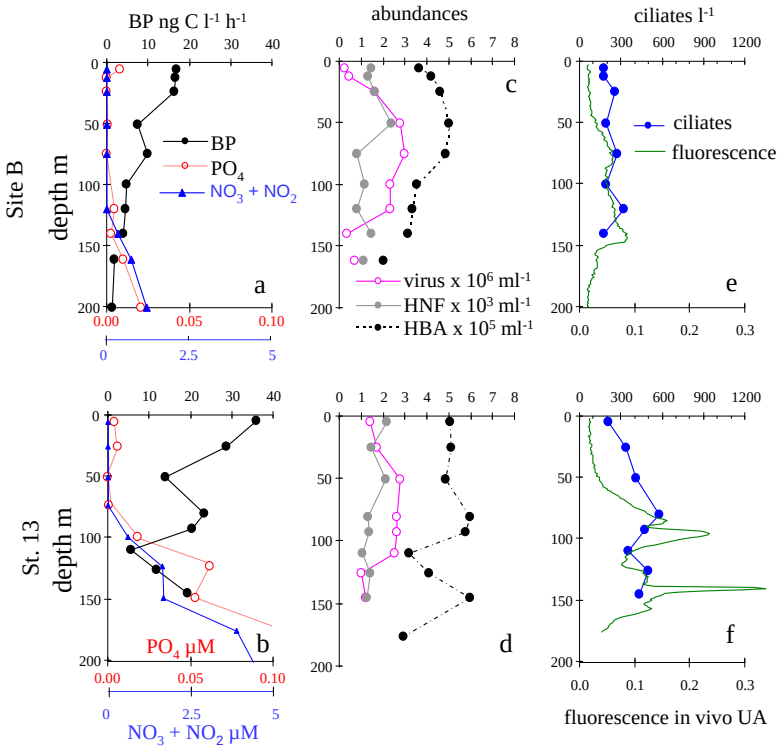

Fig. 5. Profiles of bacterial production (ng C l^{-1} h^{-1}), PO_4 and NO_2+NO_3 (µM) **(a, b)**, viral (VLP, 10^6 ml^{-1}), bacterial (HBA, 10^5 ml^{-1}) and heterotrophic nanoflagellate abundance (HNF, 10^3 ml^{-1}) **(c, d)**, ciliate abundance (l^{-1}) and in situ fluorescence **(e, f)** in the center of the eddy B (upper panel **a**, **c**, and **f**) and at St. 13 (lower panel **b**, **d** and **e**).

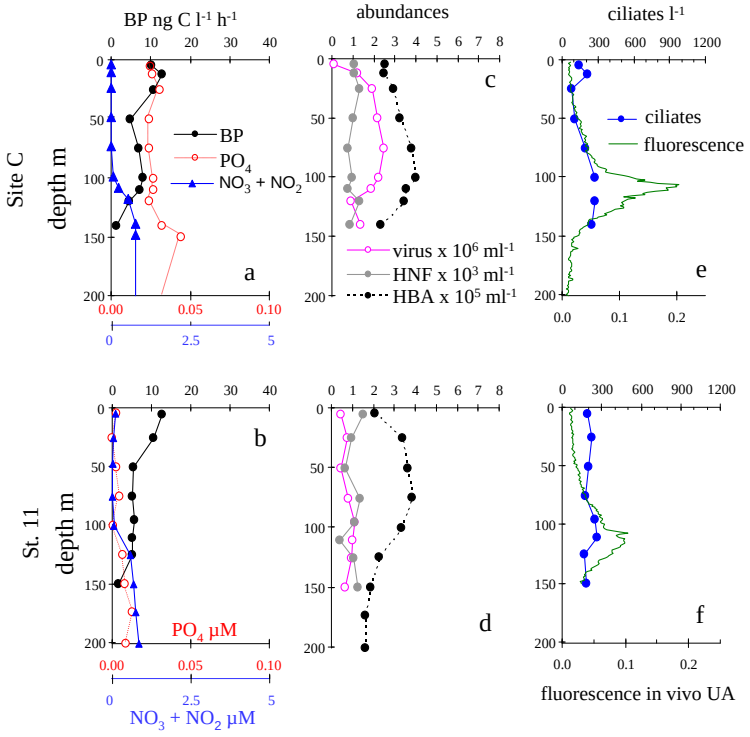

Fig. 6. Profiles of bacterial production (ng C l^{-1} h^{-1}), PO_4 and NO_2+NO_3 (µM) **(a, b)**, viral (VLP, 10^6 ml^{-1}), bacterial (HBA, 10^5 ml^{-1}) and heterotrophic nanoflagellate abundance (HNF, 10^3 ml^{-1}) **(c, d)**, ciliate abundance (l^{-1}) and in situ fluorescence **(e, f)** in the center of the eddy C (upper panel **a**, **c**, and **f**) and at St. 11 (lower panel **b**, **d** and **e**).

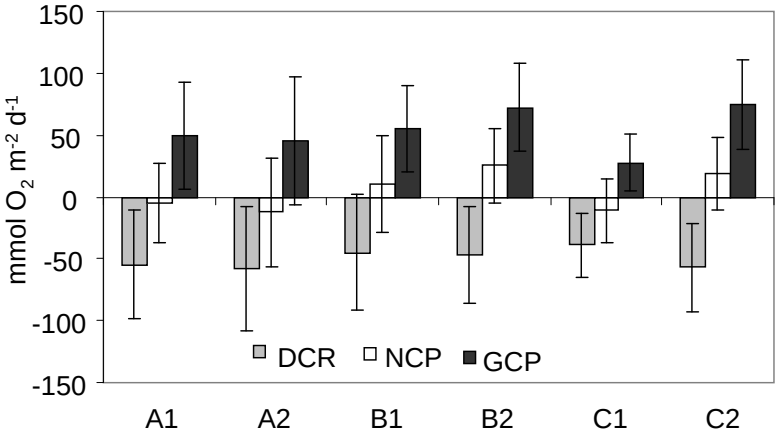

Fig. 7. Integrated GCP (Gross Community Production), DCR (Dark Community Respiration) and NCP (Net Community Production) (mmol O_2 m^{-2} d^{-1}, 130 m site A, 160 m site B, 145 m site C), at the three eddies the first (A1, B1 and C1) and the third day (A3, B3 and C3) of site occupation. Error bars represent standard deviation of 4 replicates.

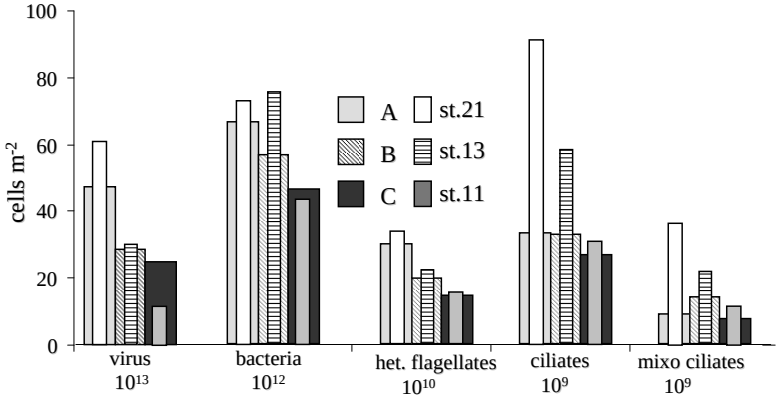

Fig. 8. Integrated values of viral particles (VLP, 10^{13} m^{-2}), heterotrophic bacteria (HBA 10^{12} m^{-2}), heterotrophic nanoflagellates (HNF, 10^{10} m^{-2}), total ciliates (CIL TOT 10^{9} m^{-2}) and mixotrophic ciliates (CIL MIXO, 10^{9} m^{-2}) abundances in the upper 150 m, inside the eddies Sites A, B and C and outside the eddies St. 21, 13 and 11, respectively.